NREL/SR-520-22565 • UC Category: 1262 • DE97000210

Atomic-Scale Characterization of Hydrogenated Amorphous-Silicon Films and Devices

Annual Subcontract Report
14 February 1995 - 14 April 1996

A. Gallagher, S. Barzen, M. Childs, and
A. Laracuente
National Institute of Standards and Technology
Boulder, Colorado

NREL technical monitor: B. von Roedern

National Renewable Energy Laboratory
1617 Cole Boulevard
Golden, Colorado 80401-3393
A national laboratory of
the U.S. Department of Energy
Managed by Midwest Research Institute
for the U.S. Department of Energy
under Contract No. DE-AC36-83CH10093

Prepared under Subcontract No. DAD-4-14084-01

February 1997

This publication was reproduced from the best available camera-ready copy submitted by the subcontractor and received no editorial review at NREL.

NOTICE

This report was prepared as an account of work sponsored by an agency of the United States government. Neither the United States government nor any agency thereof, nor any of their employees, makes any warranty, express or implied, or assumes any legal liability or responsibility for the accuracy, completeness, or usefulness of any information, apparatus, product, or process disclosed, or represents that its use would not infringe privately owned rights. Reference herein to any specific commercial product, process, or service by trade name, trademark, manufacturer, or otherwise does not necessarily constitute or imply its endorsement, recommendation, or favoring by the United States government or any agency thereof. The views and opinions of authors expressed herein do not necessarily state or reflect those of the United States government or any agency thereof.

Available to DOE and DOE contractors from:
Office of Scientific and Technical Information (OSTI)
P.O. Box 62
Oak Ridge, TN 37831
Prices available by calling (423) 576-8401

Available to the public from:
National Technical Information Service (NTIS)
U.S. Department of Commerce
5285 Port Royal Road
Springfield, VA 22161
(703) 487-4650

Printed on paper containing at least 50% wastepaper, including 20% postconsumer waste

Preface

This report describes the results from the period April 15, 1995 to April 15, 1996, carried out by the National Institute of Standards Technology (NIST) under contract DAD-4-14084-01 from the National Renewable Energy Laboratory. The research is carried out under the direction of Dr. Alan Gallagher, a NIST physicist, in "JILA" on the University of Colorado campus in Boulder, Colo. Under a subcontract with the University of Colorado, graduate students and post -doctoral students of the University work on the project. During the period covered by this report the graduate students have been: Arnaldo Laracuente, who is graduating in August, 1996, and Stefan Barzen since November, 1994. A post-doctoral student, Michael Childs joined the program in June, 1995.

Abstract

The research is concerned with improving the electronic properties of hydrogenated amorphous silicon (a-Si:H) films and of photovoltaic (PV) cells that use these films. Two approaches toward this goal are being taken. One is to establish the character of silicon particle growth in the rf glow discharges that are used to make the films and PV cells, and to understand the particle incorporation into the films. The ultimate goal of this effort is to find mitigation techniques that minimize the particle incorporation. During this contract period, we have developed a novel particle light-scattering technique that provides a very detailed and sensitive diagnostic of the particles suspended in the discharge. The second program is directed toward measuring the electronic properties of these thin-film PV cells, as a function of depth within the cell. The approach being taken is to use a scanning tunneling microscope (STM) to measure the depth-dependent electronic properties of cross-sectioned PV cells. During the present period, cell cleaving and cross section locating methods, both in a UHV environment, have been successfully developed.

Summary

Goal

The first objective of this work is to establish methods that diminish the incorporation of Si particles into the films of a-Si:H PV cells. These particles are not large enough to induce shorts, but they are sufficiently numerous to have a major effect on electrical quality. To achieve this objective we need to understand the growth and behavior of particles in the rf discharges currently used to deposit a-Si:H PV cells, and why these incorporate during film growth. Using this understanding, we will then establish methods of modifying the deposition techniques to diminish this particle incorporation.

A second part of the program is designed to measure the distributed electrical properties within a-Si:H, PV cells. The purpose is to assist manufacturers in improving cell properties. By isolating junction regions or regions within the i-layer, and measuring their behavior versus illumination and light soaking, we hope to improve understanding of where inefficiencies arise within the cells. The method employed will be STM tunneling into cross-sectioned cells in a UHV environment, versus illumination, light-soaking, etc.

Results

We have developed a novel light-scattering method that discerns particle size and position distributions within the discharge, and is sensitive to very small particle sizes. This is based on pulsed-laser scattering and independent detection of the scattering from very small volumes within the discharge. Complementary STM measurements, described in previous reports, discern the incorporation of small particles into the films. The light-scattering measurements provide uniquely detailed and sensitive information, that is being used to diagnose particle growth and trapping within a-Si:H deposition discharges. Present conditions are similar to those used for device manufacture, and severe particle buildup is discerned, particularly near the downstream end of the discharge.

The other component of our research, to measure the properties of cross-sectioned cells with the STM, is in the development stage. We have so far constructed and tested an STM and sample manipulator specifically designed to allow these measurements. This includes the ability to minimize probe perturbations by using exceptionally low (~10 fA) tunneling currents, as well as optics for sample illumination within the UHV STM. Tip approach to the very thin side of the cleaved cell is also a very tricky problem, which has been largely solved by the use of very fine sample-position manipulators and computer-controlled sample and probe manipulations. Another important step has been the development of a cleaving method that minimizes sample strain and exposes the surface only to a UFW environment.

Table of Contents

Preface	i
Abstract	ii
Summary	iii
1.Introduction	1
2. Light scattering observations	2
3. Model for particle deposition during film growth	9
4. Apparatus for cross-sectioned PV cell diagnosis	12
5. Conclusions	15
6. References	17

Table of Figures

Fig. I Schematic diagram of the scattering apparatus.	3
Fig. 2 Schematic diagram of the discharge volume.	4
Fig. 3 Images of scattered YAG laser light.	6
Fig. 4 Image of scattered YAG laser light showing individual particles.	7
Fig. 5 Images of scattered HeNe laser light.	8
Fig. 6 Diagrammatic representation of the cycle-averaged electron density (n_e^- cation density (n^+), total negative charge density (n^-), charged particle density (n_p^-), neutral particle density (n_p^o), and electric field (E) versus position between the plates of a rf parallel plate silane discharge.	11
Fig. 7 Top view of the cell holder used for STM measurements on cross-sectioned cells and the STM probe.	13
Fig. 8 Front view of the cell holder used for STM measurements on cross-sectioned cells.	14

1. Introduction

Particulate growth in plasmas is ubiquitous, and is now widely recognized as a serious problem In almost all plasma processing, in etching as well as deposition discharges. This can cause obvious deleterious effects such as device failure or shorts when >0.3 mm diameter particles deposit on the substrate. This problem has been eliminated in industrial a-Si:H, photovoltaic cell manufacturing. However, it is now clear that much smaller particles more easily incorporate into growing films, and these have more subtle effects on the film electrical properties. Silicon particulates readily form in a-Si:H deposition discharges, but they become negatively charged in the discharge and this is normally expected to trap them in the plasma and prevent their incorporation into the growing film. Thus particles have primarily been expected to be a problem when the discharge is switched off and they can reach a surface. However, we recently showed that very small particles continuously incorporate into the film during growth, and with sufficient density to potentially be the primary cause of a-Si:H film inhomogeneities and electrical defects [Tanenbaum et al. 1995, Tanenbaum et al. 1996, Gallagher et al. 1995]. This is supported by some measurements at other laboratories, which have shown a dependence of film optical properties on the presence of particles in the discharge [Schmidt et al. 1993]. Thus, it has become quite important to establish the character of particle growth and trapping in a-Si:H deposition discharges, and ultimately to decrease their incorporation into a-Si:H, PV cells.

Light scattering is the most common method of detecting particles suspended in discharges, but as normally applied it has serious limitations for the present problem. Very small particles, typically of 2-15 nm diameter (d), are incorporated into the a-Si:H film, and most of these are too small to be detected by light scattering, which is proportional to d^6 for small particles. However, a great deal can be inferred about the small particles if we can detect light scattering from slightly larger particles, which is feasible for d> 10 or 15 nm. The problem is that, due to this d^6 dependence, the total scattering is dominated by large particle scattering and the small particles are not normally observed. Thus, we need a method that obtains the entire size distribution at all spatial positions in the discharge. During this year we have achieved this, by developing a novel light-scattering method, which is described in the following section. As will be seen by the preliminary data shown there, this opens the opportunity to develop a detailed understanding of small-particle behavior in these discharges.

A second advance made during the current contract was to develop a plausible explanation for the surprising fact that small particles continuously deposit into the growing a-Si:H film. This model is described in Sec. 3.

PV cells contain several layers and junctions, and it is quite difficult to independently establish the behavior of these different components and junctions in the composite structure. A variety of sophisticated optical and electrical measurements provide valuable hints regarding the locations and causes of cell efficiency losses, but unique connections to particular locations orjunctions are not available. In this part of our program, we are attempting to develop a measurement method that can more uniquely separate the electrical behavior of each region of a PV cell. This is based

on scanning tunneling microscope (STM) spectroscopy of cross-sectioned cells. The objective is to measure the shapes and positions of the bands, and quasi Fermi levels, at all positions within an operating cell, using STM current-voltage spectroscopy across the cell cross section. For crystalline semiconductors this STM-spectroseopy method is now a well established diagnostic of semiconductor junctions, superlattices and devices (e.g. Silver et al. 1995, Smith et al. 1995, Thibado et al. 1996). However, there are several factors that make this much harder for a-Si:H PV cells. (1) Crystalline semiconductors are much better conductors than a-Si:H, so we need to work at much lower tunneling currents than is traditional and convenient with an STM. A very low current, in vacuum, amplifier has been developed for this, as described in Sec.4. (2) Crystalline semiconductors cleave along lattice planes, providing a relatively flat and passivated surface. In contrast, the cleaving of this amorphous material is untested, and we need to see if it introduces excessive surface states in the band gap. If this occurs, we plan to try hydrogen passivation of the cleaved surface to decrease surface dangling bonds. As will be described in Sec. 4, we have developed a method of relatively low stress in-vacuum cleaving, but we have not yet established the character of the surface states. (3) The a-Si:H PV cells are deposited on glass substrates, which are ~1mm thick. The STM probe must be placed over the ~1μm wide cleaved end of the cell, without passing over the non-conducting glass substrate, as the leknof feedback would then "crash" the probe. This uniquely precise "approach" between STM probe and sample has been achieved this year, and will be described in Sec. 4.

2. Light scattering observations

Light scattering from silicon particulates in silane discharges has been carried out in a variety of laboratories, but few measurements are made under "device quality" deposition conditions and the observations have not been correlated with film properties (e.g. Watanabe et al. 1990, Bouchoule et al. 1991, Fukuzawa et al. 1994, Howling et al. 1994, and Schmidt et al. 1993). In addition, the amount and location of particulates is highly dependent on the details of each individual deposition chamber. We have therefore set up light scattering observations for a discharge chamber that is as close as possible to that with which we produce films for STM studies. It is also designed to represent typical industrial confined-flow chambers, although on a smaller scale. It can be heated to a typical 250' C, but the observations reported here are at 25' C. It is worthwhile to note that we utilize the same deposition rate, hence power density, typically used for producing device-quality films, and our flow velocities are very high by normal standards (large mass flow/tubing area). Thus one expects more particulates in most silane PECVD chambers than are reported here.

In conventional light scattering experiments, the total intensity, or intensity and polarization, of the scattered light is measured. This measurement is not sufficient to determine the size distribution. Also, it will be disproportionately influenced by the larger particles, as noted in the introduction, because the scattering cross section for particles smaller than $\lambda/2\pi$, where λ is the wavelength, is proportional to d^6. However, the smaller particles deposit into the film, so it is important to measure the full size distribution. Our method, shown in Fig. 1, detects light

scattered from individual particles, and consequently establishes the size distribution at all positions in the discharge. A frequency-doubled YAG laser beam (532 nm) is formed into a thin sheet and sent through the rf plasma, where a small fraction is scattered by the particles. This scattered light is imaged onto a CCD camera. Thus, each CCD pixel detects the light scattered from a small volume of the plasma. Since the YAG pulse duration is short enough to freeze the particle motion, a snapshot of the particles is observed. Provided that the plasma volume imaged onto a pixel contains on average less than one particle, the particles are detected separately. This is an important advantage since it prevents the signals from larger particles from obscuring the smaller-particles signals by spatially segregating the signals. Particle density is found by simply dividing the number of observed particles by the total imaged volume. Particle size is determined from Mie scattering theory, assuming spherical particles. The signal size is calibrated by comparison to Rayleigh scattering from an atmosphere of nitrogen. Under optimal conditions, this apparatus is capable of detecting particles with d $\geq$25 nm.

Our apparatus, shown to scale in Fig. 2, has been operated with 8-10 sccm of pure silane gas at 250-300 mTorr. (This is a flow of ~0.9 sccm/cm^2, which is equal to or larger than the flow speed used in most industry systems.) The electrode assembly is inside a cylindrical tube to assure that the gas flows between the electrodes, but holes are cut in the tube to allow collection of scattered light. The applied rf voltage is 130 V peak-to-peak, and the film growth rate is ~1 Å/s.

A series of images of the particles observed by scattering of the YAG laser light are shown in Fig. 3. For these images, the silane flow was 10 sccm at 314 mTorr. The location of these images is indicated by the small image region in Fig. 2 at the downstream edge of the rf electrode, midway between the electrodes. TheYAG beam has a widthof ~30μm, duration of ~10 ns, and pulse energy of ~200 mJ. Clearly, over the first minute of plasma operation the dust particles are numerous in this region and they retreat downstream with increasing discharge time, After a minute, no further signal is apparent at this location. Because the particles are so numerous in this region, individual particles are not easily resolved. The minimum particle density, determined by the resolution of the apparatus, is ~3x10^8 cm^{-3}. The range of intensities of the barely resolved individual particles at the edge of the particle field correspond to particle diameters of about 25-35 nm.

Individual particles are apparent in Fig. 4. This image was obtained under conditions essentially the same as those images shown in Fig. 3, but on another occasion. This image was taken 10 minutes after the discharge was lit. The fact that particles are still present illustrates that the behavior of the particles is sensitive to many factors, not all of which are understood or have even been identified. The particles in this image are about 30-40 nm in diameter. A cw HeNe laser beam shaped like a ribbon similar to the YAG beam has also been used to study the particles in the plasma. Due to particle Brownian motion, images of moving particles are normally smeared when using the HeNe laser and this method is not appropriate for identifying small (i.e. quickly moving) particles. However, the HeNe laser has the advantage we can gain additional information about the time dependence of the various features. Figure 5 shows several images taken with the HeNe laser beam. The top row shows the evolution of the dust particles over the initial few minutes for a silane gas flow of 10 sccm at 310 mTorr. I nitially, the dust is

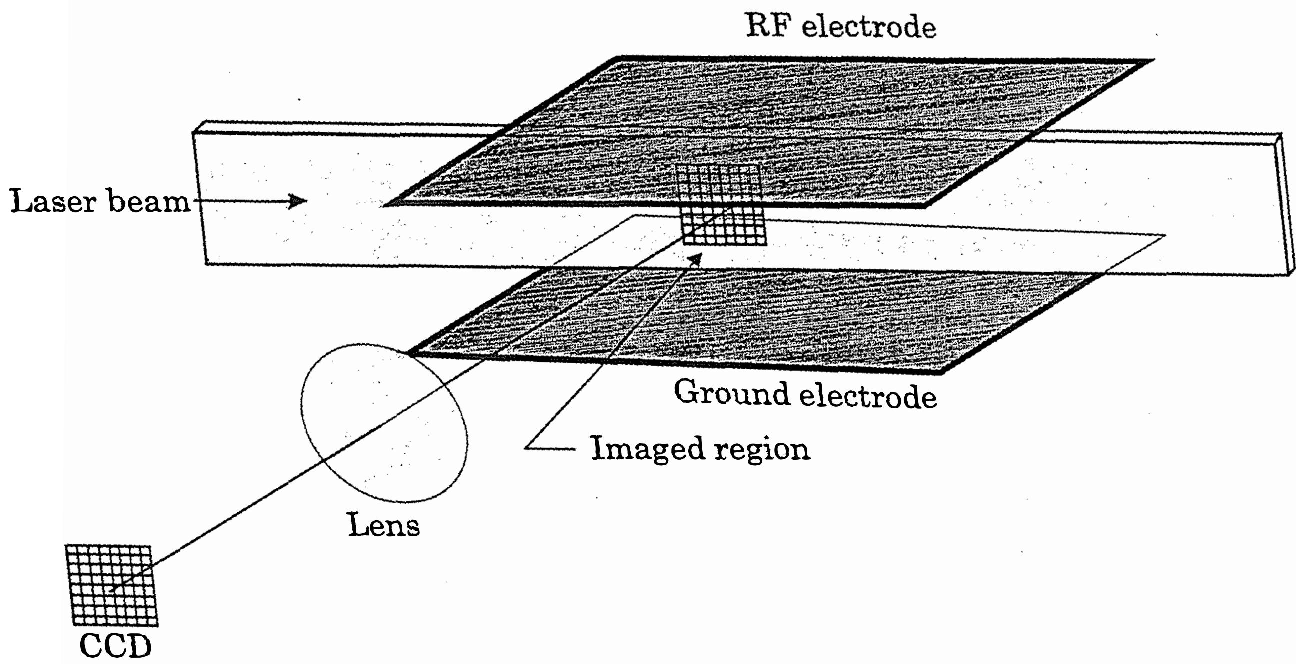

Fig. 1. Schematic diagram of the scattering apparatus. Light scattered from different regions of the plasma are detected separately, which allows the distribution of particle sizes to be determined.

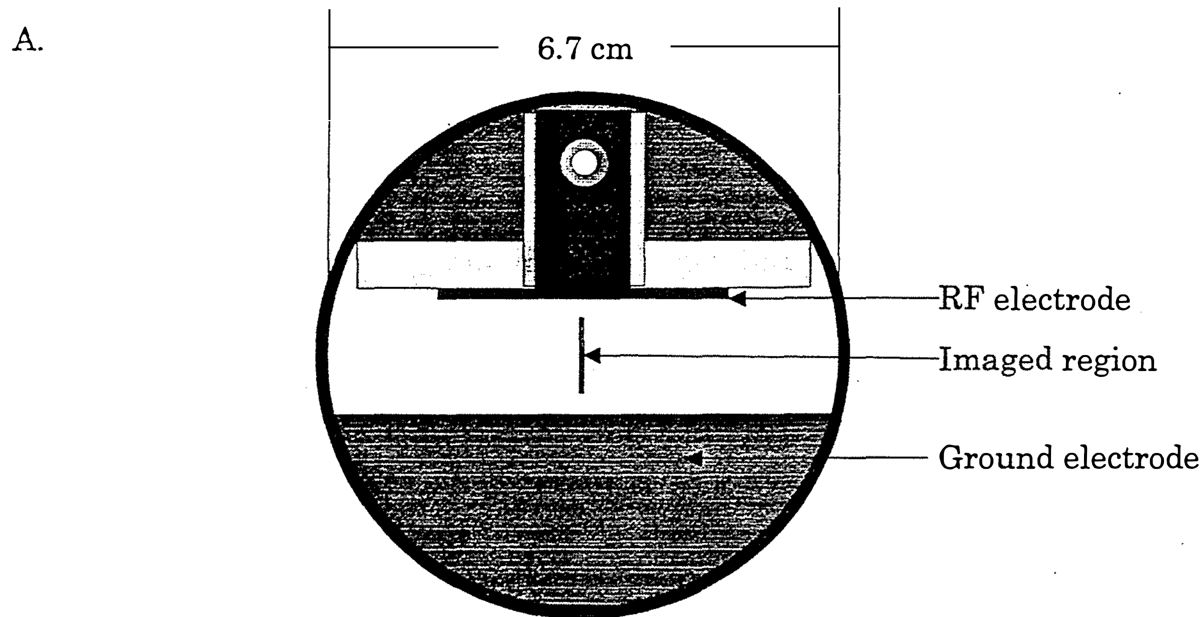

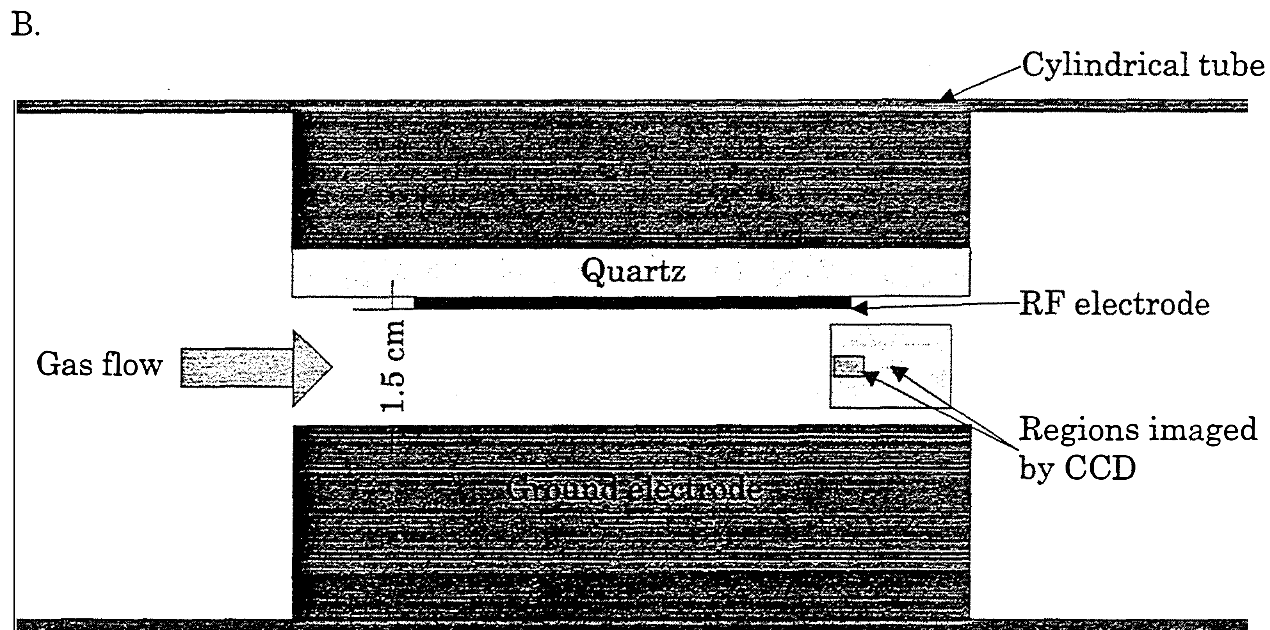

Fig. 2. Schematic diagram of the discharge volume viewed (A) in cross section from the end and (B) from the side. The regions imaged by the CCD are indicated; the larger and small regions were monitored using a HeNe and YAG laser beam, respectively.

between the electrodes and in the region just downstream of the electrodes. After a minute, the dust has been pushed out of the discharge region by the gas flow and is solely in the downstream region. After 8 minutes, the dust settles into a fairly stable configuration even further downstream. Small changes in gas flow and pressure result in the dust cloud changing configuration, as seen in Fig. 5d where the dust forms two bright and stable groups followed by a dim tail. Even more startling, the dust can form "plasma crystals" at slightly lower flows and pressures (Fig. 5e-f). In the crystal configuration, particles separated by ~200μm perform small oscillations about stable nodes. Several forces are involved in forming these crystals, though the details are far from clear. The particles are pushed downstream by viscous drag, but are prevented from leaving the positive plasma by electric fields. Evidently, the Debye length in this region is long enough that the particles are able to interact with each other, resulting in the fairly uniform particle spacing. Such "plasma-particle crystals" have been previously observed, although the plasma crystal observed here is unique in several ways: the particles are grown *in situ* (instead of being seeded), gas drag is a significant force, and the apparatus is similar to those used for industrial a-Si:H film growth. We believe that this is the first time that plasma crystals have been observed under these conditions.

3. Model for particle deposition during film growth

In order to mitigate the deposition of small particles into the growing a-Si:H film, it would be very helpful to have a model for why these particles are depositing into the film. Available discharge and particle models predict that particles are suspended in the plasma during the discharge, so it is necessary to develop an improved understanding of particle behavior in discharges. Here we first describe current understanding of particle behavior in plasmas, then the model we have developed for the cause of this surprising particle deposition during the discharge.

Since electron velocities are much greater than cation velocities in a discharge, yet the cycle-averaged + and - charge losses to the surfaces must balance, a rf discharge plasma becomes positively charged by an average voltage of typically 1/2 the peak voltage or 40 V. This reduces the electron current and increases the cation current to the electrodes. This voltage drop, or equivalently a large electric field, appears near the electrodes as shown by the electric field in Fig. 6a. This large field region is called the sheath, and the region of nearly equal + and - charges in the center is called the plasma. (Rf-cycle averaged fields and charge densities are shown in Fig. 6 only these are relevant here since particles move very little during an rf cycle.) A particle within the plasma behaves as another surface, to which the average + and - currents must also balance. To achieve this the particle surface also acquires a negative voltage relative to the surrounding plasma, by carrying a net negative charge. Since the particle potential can oscillate with the plasma potential during the rf cycle, it only needs to acquire a negative voltage of 2-3 kT_e, typically 5-10 V. This typically requires a number of negative charges $N \cong 2(d/nm)$, where d is the particle diameter. For the 2-15 nm particles we found deposited in the film, this implies $N \cong 4$-30. Particle kinetic energies are essentially thermal at the gas temperature, so no negatively

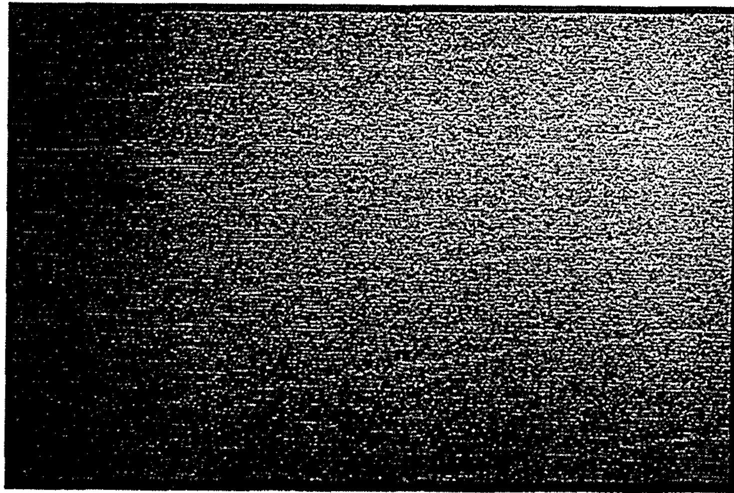

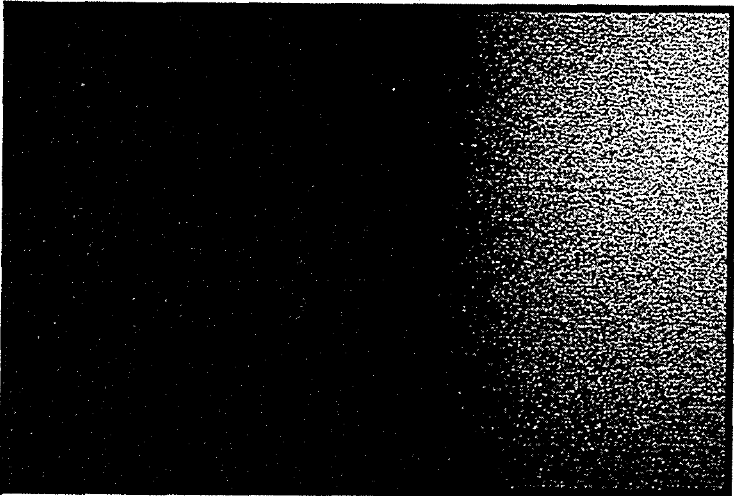

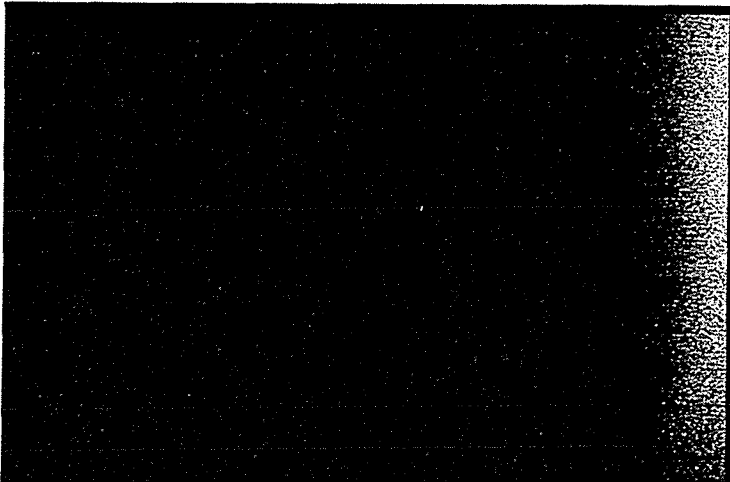

Fig. 3. Images of scattered YAG laser light taken at the downstream edge of the rf electrode midway between electrodes, as indicated in Fig. 2. Gas flow is from left to right. The top, middle, and bottom images were taken approximately 20, 35, and 50 seconds after the discharge was lit, The imaged area is 4 mm wide and 2.7 mm tall. The horizontal and diagonal lines are artifacts produced by the CCD.

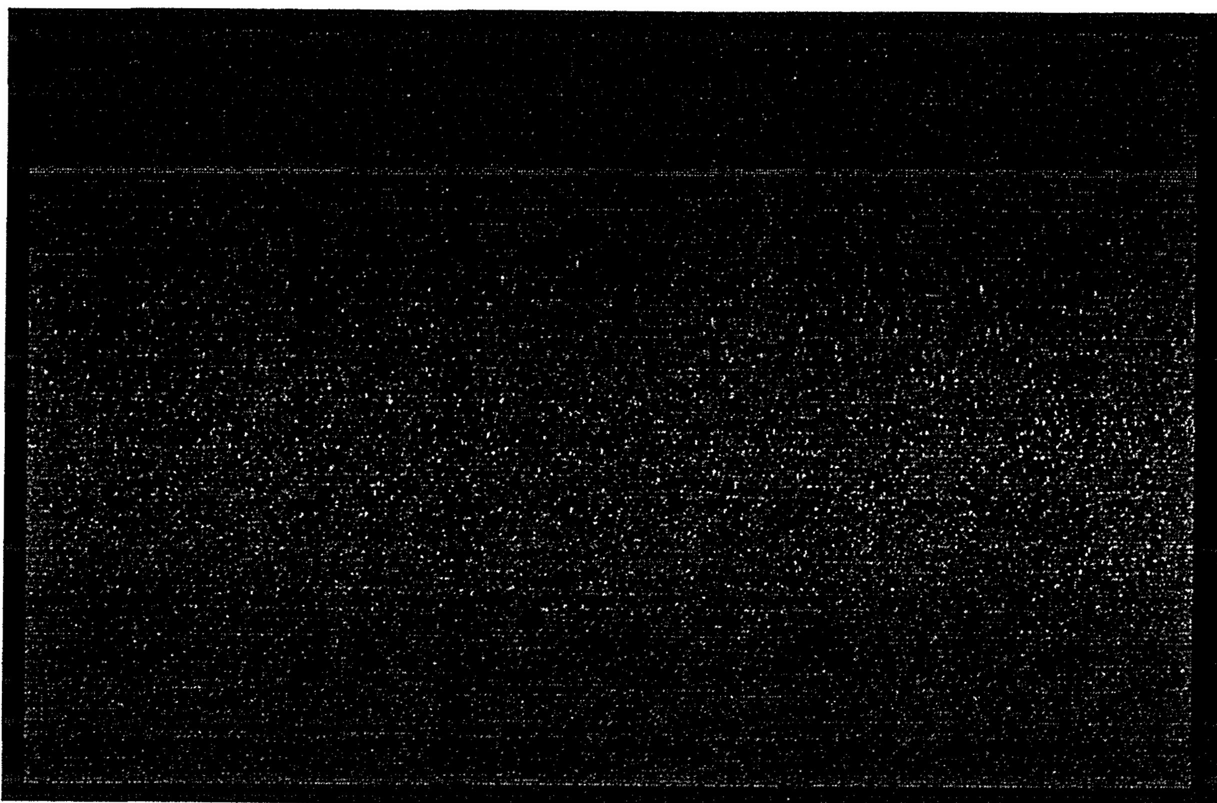

Fig. 4. Image of scattered YAG laser light. The individual particles that are apparent on the edges of this image are ~30 nm in diameter.

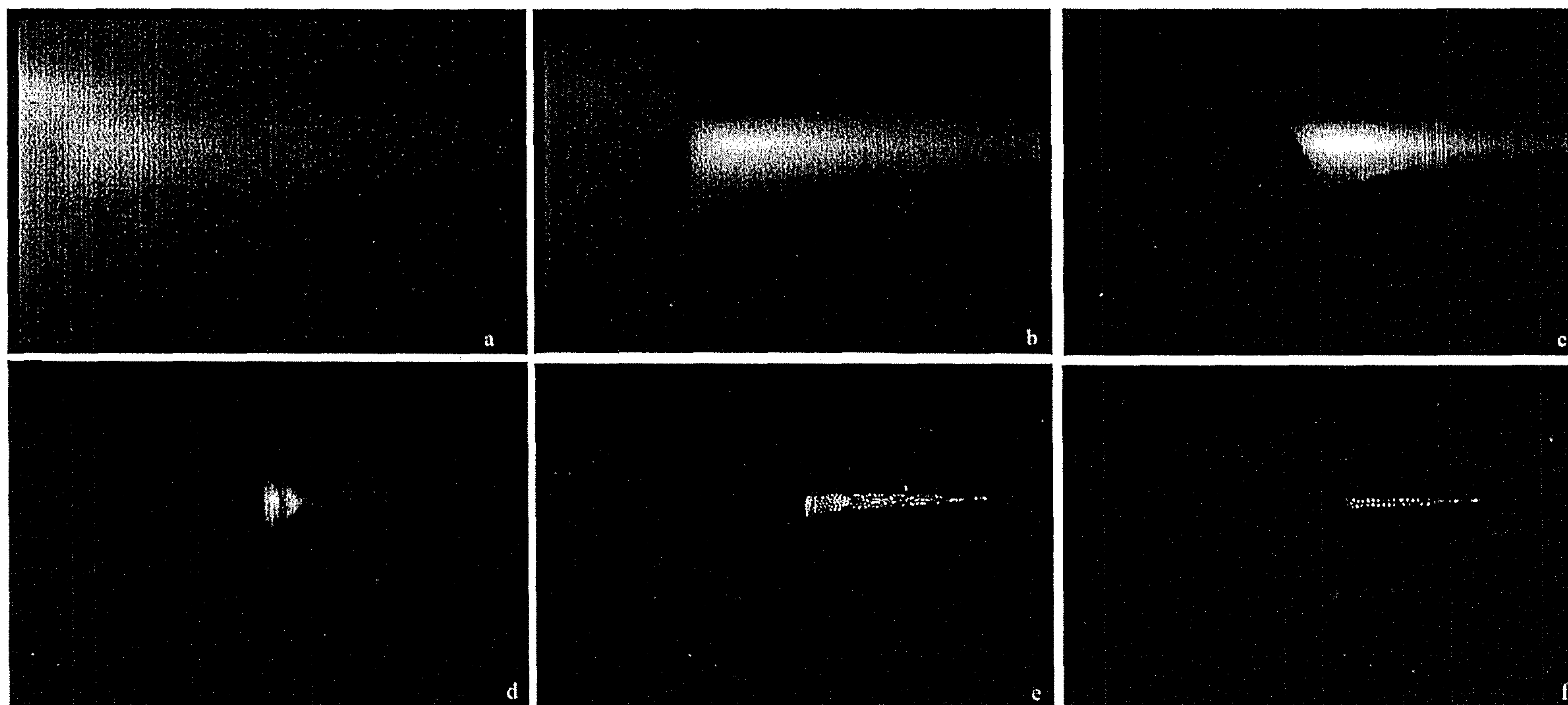

Fig. 5. Images of scattered HeNe laser light taken at the downstream edge of the rf electrode, as indicated in Fig. 2. The region imaged is 10.7 mm tall and 16 mm wide; each image is a 0.1 sec exposure, although the brightness of the images has been adjusted to make the images clearer. The top three images show the evolution in time of the dust cloud for a gas flow of 10 sccm at 310 mTorr(a) ~30 sec., (b)~60 sec., and (c) 8 min. After the discharge began. At slightly lower pressure and slower gas flow (270 mTorr and 9 sccm), the dust cloud in (d) is a stable configuration. By reducing pressure and flow to 244 mTorr and 8 sccm, the particles arrange themselves into a crystal (e) which over several minutes transforms into (f). Some of the brightness variations in (e) and (f) in the middle of the crystal are because the plane of the laser beam does not exactly match the crystal plane.

charged particles can pass through the very strong sheath electric field, or even the weak electric field at the sheath-plasma boundary. Cations produced in the plasma and accelerated toward the sheath undergo Coulomb collisions with the particles, producing an "ion wind" force that pushes the particles against the plasma-sheath boundary, to the positions shown in Fig. 6a.

Discharge models have shown that particle charge fluctuations around the average value are nearly characterized by a Gaussian (Poissonian for small N) behavior with variance of $N^{1/2}$, so only a very small fraction of the particles will be neutral and most of these will be the smallest particles. Furthermore, electron collisions with a neutral particle are $>10^2$ times as frequent as cation collisions, and this will rapidly recharge any particle that momentarily becomes neutralized. This charging time is much less than the time required for a particle to diffuse across the sheath to the substrate, and we calculate that a probability of $<10^{-10}$ for a 5 nm particle to diffuse to the substrate without encountering an electron, charging and being returned to the plasma region. Thus, it appears that particles should not reach the substrate during the discharge at anywhere near the quantities or sizes that we observed. In essence, this is the natural conclusion that has previously been drawn from currently accepted discharge-particle models.

To explain the particle fluxes we observed incorporating from the discharge into the a-Si:H film, two factors must change: (1) a larger fraction of the particles suspended in the plasma must be neutral, and (2) the probability of a particle traversing the sheath must be higher. A likely cause of the first factor is large particle densities at the sheath edge, such that a large fraction of the negative charge resides on particles rather than electrons. This is shown in Fig. 6b, where n_p^- represents the net charge density on particles and n_e^- the electron charge density. Under these circumstances, the electron and cation currents to the particle balance for a much smaller negative voltage on the particle, or equivalently a much smaller average negative charge. The Poisson distribution of charges then contains a significant (>1%) component of neutrals for sizes below 15 nm. This is a reasonable explanation of factor (1), allowing sufficient neutral particles to diffuse into the sheath region as shown in Fig. lb, but how do these traverse the sheath?

Due to their weight and size, neutral particles diffuse slowly. The probability of diffusing across the sheath without being recharged by an electron collision is $Tr=\exp(-\langle R_e / D_p\rangle^{1/2} W)$, where R_e is the electron collision rate, $D_p = v_s/(3\, n_s\, Q_p)$ is the particle diffusion rate, W is the sheath width, v_s and n_s refer to the silane and $Q_p=\pi d^2/4$ is the neutral particle cross section. As already noted, Tr is less than 10^{-10} for a 5 nm particle under our discharge conditions, and furthermore it is strongly dependent on particle diameter d. Both predictions are contradicted by our data. The key to the riddle of how particles traverse the sheath appears to be the following. Electrons collide with a neutral particle with the rate $R_e=n_e^- v_e Q_p$, and cations collide with a rate $R^+=n^+ v+ Q_p$. In the sheath n^+ is slightly larger than n_e^-, and $v_e / v_+ \cong 500$, so almost all particles will become negatively charge by an electron collision and be returned to the plasma. But about 0.2% of the particles will first encounter a cation and become positively charged. In the very strong sheath electric field, a positively charged particle will be rapidly driven to the substrate surface, before it has time to encounter an electron. Thus, the sheath transmission probability $Tr \cong 0.002$, and this is independent of particle size! The net flux of particles, of size d, to the substrate is thus given by $F(d) \cong n_p^\circ(d)\, Tr/t_d(d)$, where n_p° is the neutral particle density (per unit area) at the

plasma sheath boundary, as shown in Fig. 6b and t_d is the particle diffusion time into the region of strong electric field. A detailed comparison to our measured distribution of particle sizes requires knowledge of $n_p^-(d)$, which is not known, but an estimate of F(d) yields a good approximation to particle flux that we find is incorporated into our a-Si:H films.

So, does this new model suggest that particle incorporation into films is inevitable, or is it preventable? It is not possible to avoid a very large rate of negative ion production in silane discharges, since this results from about one in each 10^4 electron-SiH_4 collisions. A significant fraction of these SiH_n - ions will grow in size, due to radical and cation collisions, and once they attain 1-2 nm size they will usually be negatively charged as described above. Thus, it appears difficult to avoid a large effective rate of producing 1 nm particles. It may be possible to prevent these from growing to the 2-20 nm size range, for example by modulating the discharge and allowing the <2 nm particles to leave periodically (e.g. Watanabe et al. 1990). However, many of these small particles will deposit into the film, probably with undesirable consequences. A more desirable mitigation method would be to prevent the total particle density from growing to a critical size that yields $n_p^- \cong n^+$ at the plasma-sheath boundary; then very few particles will be neutral and capable of diffusing into the sheath. If one can find ways to extract moderate size (e.g. 100 nm) particles at the downstream end of the discharge, this should prevent the buildup of this critical particle density. Some methods have been used successfully to extract somewhat larger particles from wafer-etching plasmas; an example is to put a groove into the electrode, leading to the edge; this modifies the sheath potential that normally keeps particles from escaping. Our observations in a flowing silane, rf deposition discharge using conditions typical for the industry indicate that, in the absence of a particle mitigation procedure, particles only escape the plasma once they attain fairly large size, typically 500 nm. Thus, it appears likely that we can do a lot better.

In summary, we now have a model for the cause of particle escape from rf silane discharges, resulting in particle incorporation into growing a-Si:H films. The model invokes a high density of particles at the plasma-sheath boundary, allowing some particles to become neutral and enter the sheath. There a small but significant fraction become positively charged and are swept to the substrate by the sheath electric field. This model suggests that it should be possible to prevent much of this particle incorporation, as well as what must be done to achieve this.within the plasma behaves as another surface, to which the average + and - currents must also balance. To achieve this the particle surface also acquires a negative voltage relative to the surrounding plasma, by carrying a net negative charge. Since the particle potential can oscillate with the plasma potential during the rf cycle, it only needs to acquire a negative voltage of 2-3 kT_e , typically 5-10 V. This typically requires a number of negative charges $N \cong 2(d/nm)$, where d is the particle diameter. For the 2-15 nm particles we found deposited in the film, this implies $N \cong 4$-30. Particle kinetic energies are essentially thermal at the gas temperature, so no negatively charged particles can pass through the very strong sheath electric field, or even the weak electric field at the sheath-plasma boundary. Cations produced in the plasma and accelerated toward the sheath undergo Coulomb collisions with the particles producing an "ion wind" force that pushes the particles against the plasma-sheath boundary, to the positions shown in Fig. 6a.

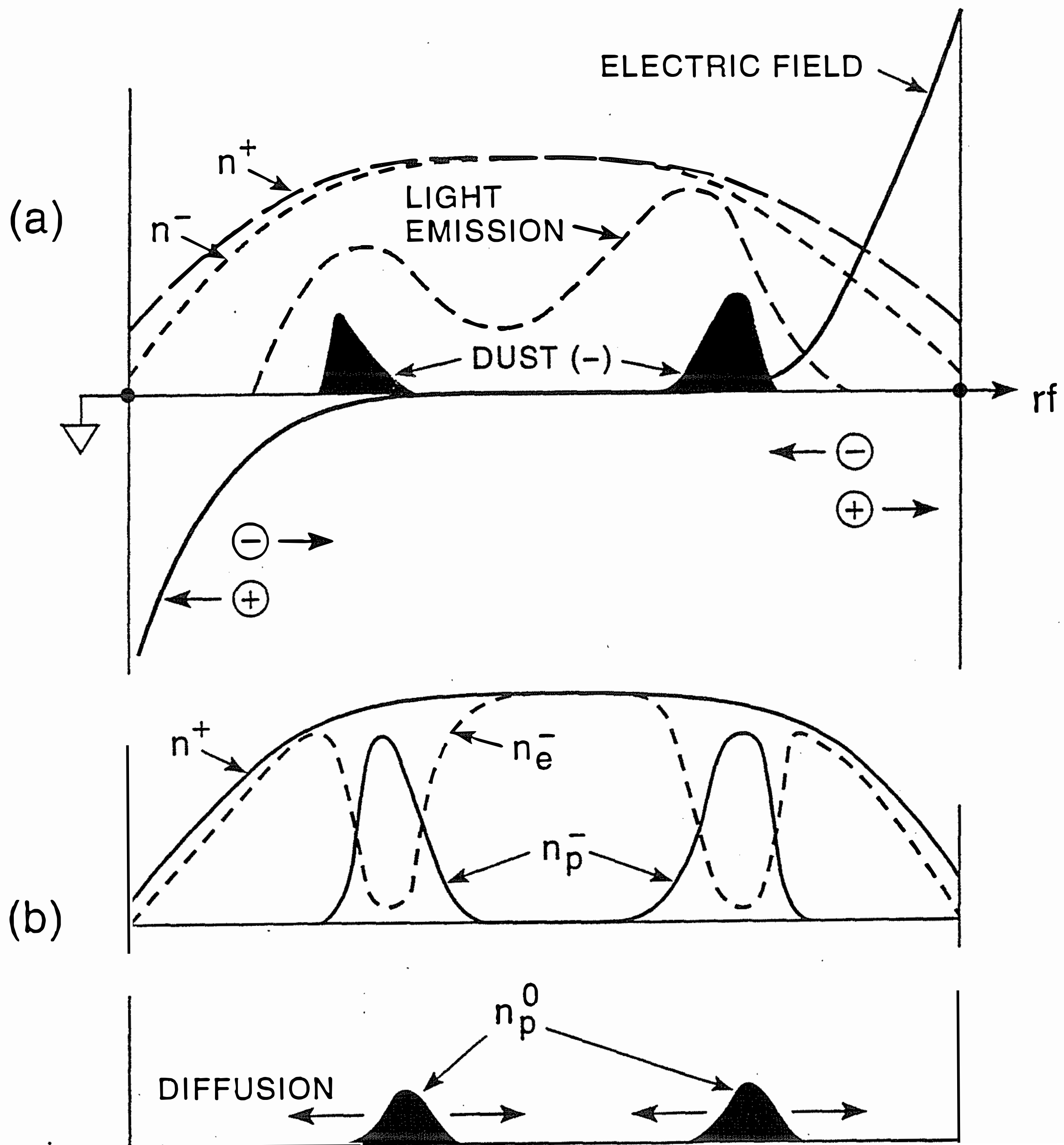

Fig. 6 Diagrammatic representation of the cycle-averaged electron density (n_e^-), cation density (n^+), total negative charge density (n^-), charged particle density (n_p^-), neutral particle density (n_p^o), and electric field (E) versus position between the plates of a rf parallel plate silane discharge. A typical pressure of 0.5 Torr, gap of 2 cm, and deposition rate of 0.15 nm/s is being represented, where the peak charge densities are ~3×10^8 /cm^3. The arrows in part (a) represent the direction of the electric-field force.

4. Apparatus for cross-sectioned PV cell diagnosis

The technical objective of this activity is to measure the electrical properties of a-Si:H PV cells, as a function of the depth within the cell and of illumination and light soaking. When a metal STM probe is placed -0.5 nm above a semiconductor surface, electrons can tunnel across the gap from filled to empty states. As the voltage difference between sample and probe (V) scans past the semiconductor band edges, the current rapidly increases due to the increasing state density. Using positive and negative polarities, the band edges and Fermi or quasi-Fermi levels can thus be observed, in principle. This current vs. voltage data is normally called "STM spectroscopy." Since the STM probes a <1 nm spot on the surface, this can be a very local probe, and by placing the probe above different regions of the cleaved cell surface, one can, in principle, establish the voltage positions of the band edges throughout the operating cell. However, in practice this is a very difficult process, and we are not certain we will be successful in applying it to a-Si:H cells. The most encouraging factor is that this has already been done for crystalline superlattices and p-n junctions (e.g. Silver et al. 1995, Thibado et al. 1996). However, these are much easier to deal with than an a-Si:H PV cell, and our efforts have been directed towards overcoming the differences. There are three primary differences which we must overcome, and our efforts are outlined in the following paragraphs. This work is being carried out by Stefan Barzen, using a homemade STM. This has the advantage that this STM can be dedicated to this effort, but it also has the disadvantage that it does not always work reliably and sometimes needs additional development.

The first major difference between a-Si:H and crystalline semiconductors is the much smaller conductivity of the former, particularly for the intrinsic layers. The standard STM sends a tunneling current (I) of 0.1 - 1nA into a ~0.5 nm region, and this enormous current density can induce a voltage drop in the semiconductor due to due to space charge. In practice, one finds that demanding this current at too low a voltage places the STM probe in contact with the sample, reducing the probe to a metal-contact Shottky barrier and often placing atomic debris on the probe that confuses further measurements. This does not totally prevent useful and interesting measurements, but they cannot be interpreted with the vacuum-tunneling picture. The obvious way to correct this difficulty is by lowering I, but one must also use I-feedback to maintain the probe-sample spacing while scanning the surface and low currents are very noisy. The solution is to scan at higher V and I, and lower both only when carrying out "spectroscopy" at a fixed position. With this capability in mind, we have developed and operated an amplifier which has a noise level of ~2fA/(Hz)$^{1/2}$. This operates at the STM head, in the UHV, as it must to avoid electrical noise pickup and stray capacitance that destroys the bandwidth. The principle difficulty we find in operating with this very sensitive amplifier is that it is very easily destroyed by high V pulses (~20V) that we sometimes apply to clean debris from the probe tip.

The next major difference between crystalline semiconductors and these a-Si:H, PV cells occurs in the cleaving. Crystals tend to cleave along the weakest crystal plane, leaving a relatively flat and unstrained surface. This surface reconstructs, usually leaving surface states that are in the bandgap and produce band bending at the surface. That junctions and superiattices have been

nonetheless observed above these cleaved surfaces by STM spectroscopy is due to nearly-equal band bending for all layers, or the good fortune of relatively few surface states in the gap, or surface passivation. Cleaved glasses also can have flat surfaces, so a-Si:H may also cleave a relatively unstrained cleaved surface. The cells we are using have indium-tin-oxide (ITO) on glass, with the a-Si:H layers on this and a final Au/Pd top contact. Thus, the cleave must pass through all layers, where the ITO and the a-Si:H are each ~0.5 μm thick. After studying cleaved surfaces and edges of glass, ITO-covered glass and complete cell structures, using a SEM, we have developed a cleaving method that appears to yield relatively flat cell surfaces and sharp corners. The essence of the method is to precleave the glass in air, using the glassblowers technique of sudden hot-wire heating of a scratch to thermally strain the glass. This cracks the glass through to the ITO, but does not separate the two segments. After loading in UIIV, the cell is then cleaved by a sideways force that stretches the cell until it suddenly cleaves adjacent to the glass crack. We have now STM scanned these cleaved cells, and generally find a relatively flat and smooth surfaces on a nm scale, although the ITO part has ~20 nm roughness due to the micro crystal nature of the ITO. Thus, this appears to be a satisfactory solution to this problem, although we have not yet established the surface-state character of the exposed a-Si:H surface.

The third major difference between these PV cells and the crystal materials that have previously been studied is that the cell is a very thin conducting layer on a nonconducting substrate. The STM must tunnel only on this conducting layer, as it will "crash" into the glass if it operates in the normal I-feedback mode above a nonconductor. This requires a very unusual and careful tip-approach mechanism, to find the end of the cleaved cell. The cell holder is shown in two views in Figs. 7 and 8. The sample coarse x and z positions are controlled with "inchworms", and fine positioning is with piezoelectric crystals. The approach is done by placing the probe ~50μm to the side and beyond the cell, as shown in the top view, using optical imaging. Then, under computer control, the cell is moved sideways until it contacts the probe. A brief scan then establishes the probe slope at contact. If this is a high slope, indicating contact between the cell corner and the side of the probe, the probe is backed away 1 μm, and the cycle is repeated until a low slope indicates that the probe is scanning the cleaved end of the cell. In this way the probe "rounds the comer" of the cell without encountering the nonconducting glass surface, typically in ~30 minutes. A problem with the present form of this approach method is that the corner of the cell may be covered with loose atomic material, from the cleave, and some of this may attach to the probe tip when it scans over the comer. We are currently evaluating this issue and devising mitigating methods in case it is a serious problem.

In summary, we have now successfully developed cleaving and tip-approach methods, and a low-current STM spectroscopy capability, and we are starting to scan the cleaved surfaces of cells. Probe cleanliness and sample passivation are now the principle issues to be resolved.

5. Conclusions

This contract period has been largely used to develop new measurement capabilities; the

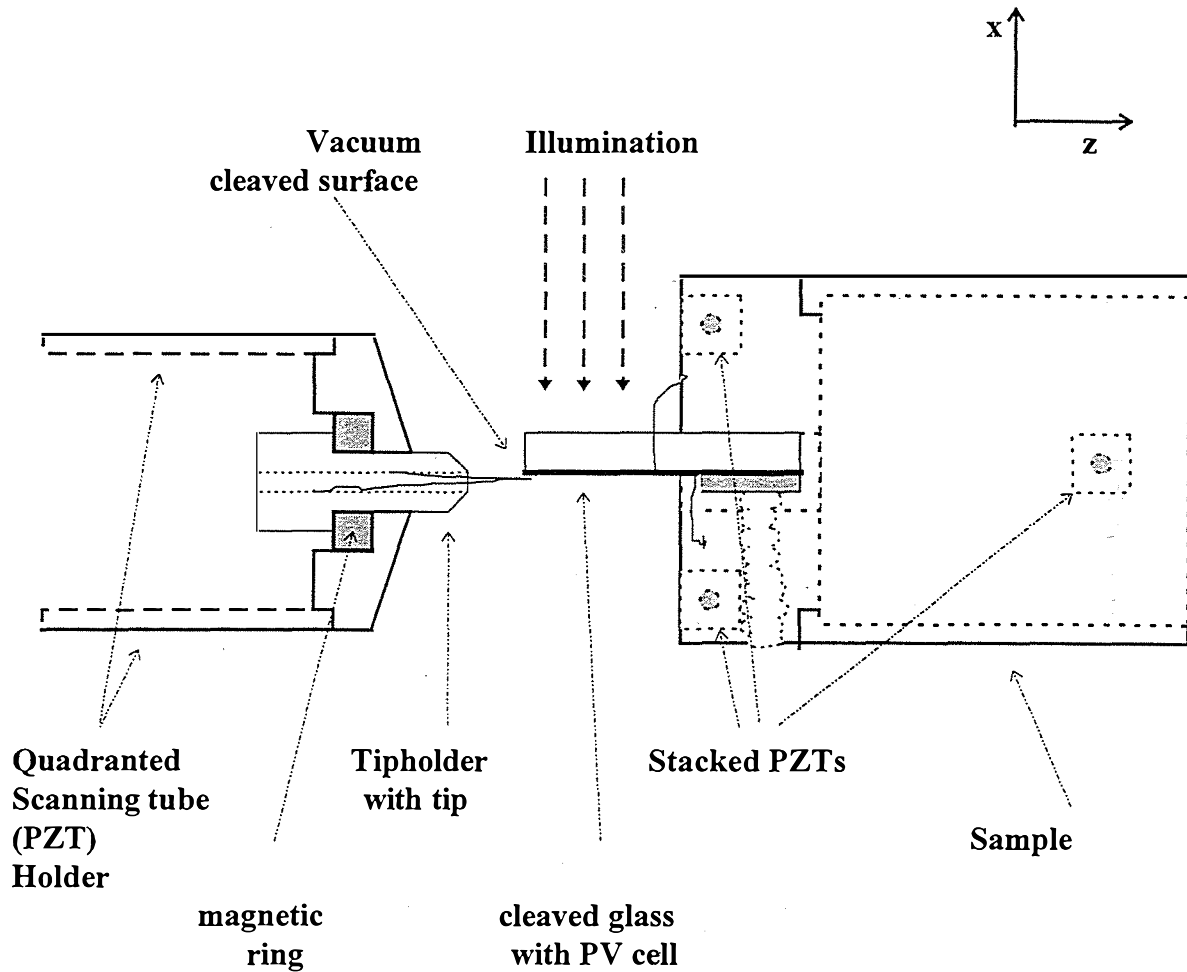

Fig. 7. Top view of the cell holder used for STM measurements on cross-sectioned cells, and the STM probe. The probe scan and final approach is provided by the quadranted PZT cylinder.

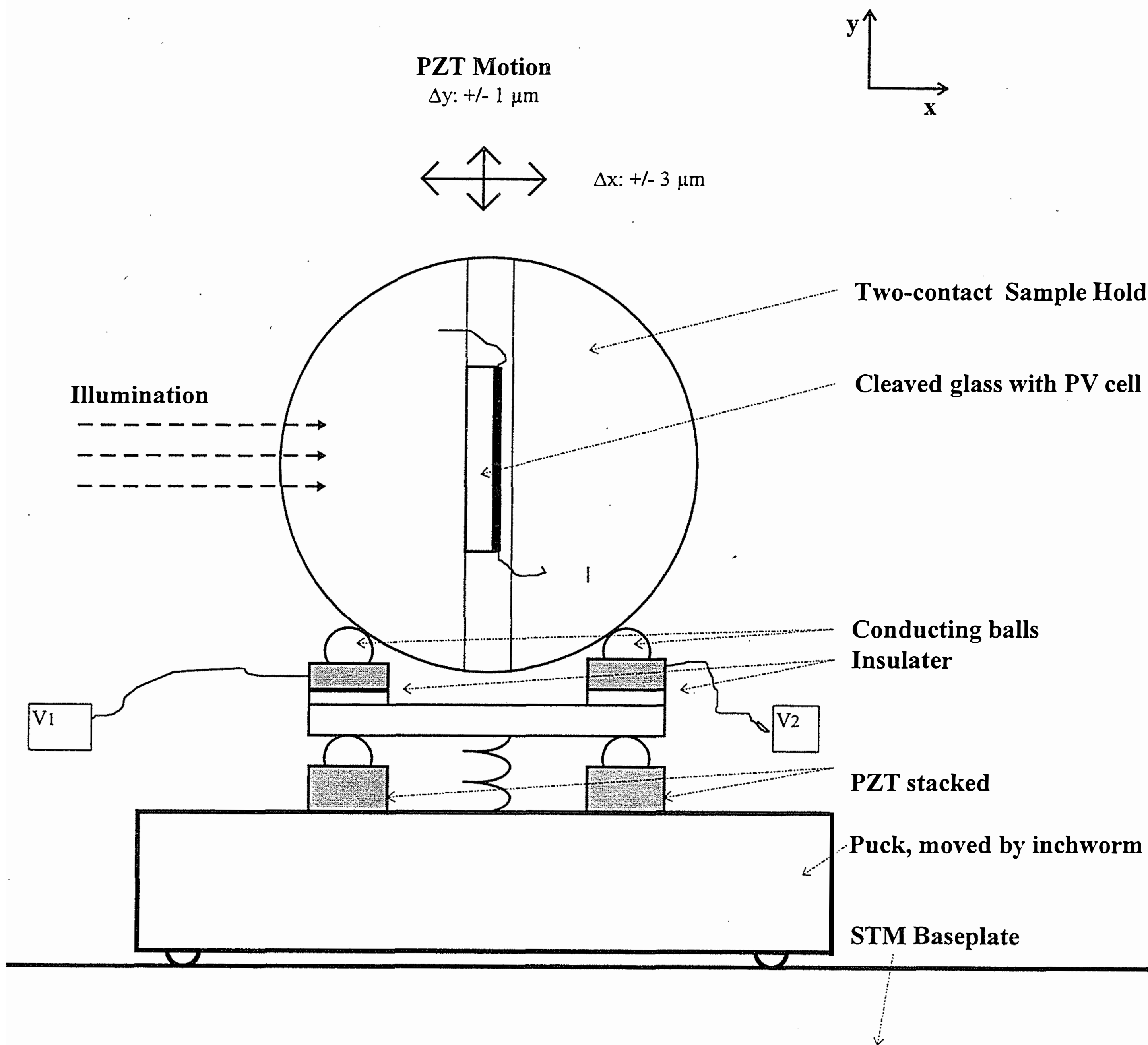

Fig. 8 Front view of the cell holder used for STM measurements on cross-sectioned cells. The cell is held between two halves of the cylindrical holder, and the cell electrodes are connected through these electrically-isolated halves and conducting support balls to the external voltages V_1 and V_2. The PZT stacks provide fine horizontal motion, by tipping the sample holder, and coarse x and z direction motion is provided by "inchworm" sliding of the "Puck". The cell-holder cylinder is 1.3 cm diameter and other dimensions are to scale, except for an exaggerated cell and glass substrate thickness.

exception is the development of a qualitative model for understanding particle incorporation into growing films. One of these new measurement capabilities, the detection of particles suspended in the discharge, is now fully operational. Also, it has achieved the full sensitivity and diagnostic capabilities for which it was designed. Using this capability, we have so far measured silicon particles at the downstream end of the electrodes, where particles are most dense and easily detected. However, we also have the capability of detecting d> 25 nm particles between the discharge electrodes, where they can be most damaging to a-SI:H devices. This will be the thrust of the measurements as soon as the behavior at the downstream end is better understood. As we expand to measurements between the electrodes, we cannot detect the very small particles that incorporate into the film by light scattering, but there is a good possibility that understanding and controlling the larger sizes that can be detected will mitigate this small-particle incorporation. Our model for small-particle (d< 15 nm) incorporation into the growing films finds that the accumulation of negative charge on larger particles is a crucial element of this small particle escape to the film. Thus, the behavior of all particles is intimately connected, and we need to understand and control them all in all regions. We conclude here that we have made major steps toward the essential experimental capability, and it is now necessary to carry out and analyze a more complete set of measurements.

The second measurement capability being developed has great potential for film diagnostics, but is much less certain of success. This STM measurement of cross-sectioned cells has been shown to work for crystal junctions, but is much more difficult for these very-thin, low-conductivity, a-Si:H Pvcells. We have made major progress in the developing crucial experimental capabilities, but still cannot predict success. The crucial issue is the quality of the cleaved, or cleaved and H-passivated surface; this will determine band distortions by surface states, as well as our ability to tunnel into the band edges. We have not yet achieved the low-voltage tunneling that is needed, but this is attributed in large part to only partial success in the difficult problem of approaching without "crashing" or getting material on the probe tip. Our computer-controlled approach still has a problem with rounding the comer without crashing, and overcoming this is our current thrust. In conclusion, considerable progress has been made, but crucial hurdles remain.

The model we have developed this year, for the cause of small-particle incorporation into the growing films, is very useful. In particular, if a large fraction of the plasma electron density at the sheath edge resides on particles, then particles can escape across the sheath to the surface. This implicates particles of all sizes in the problem, and offers the possibility of preventing this small-particle escape by minimizing the density of larger particles, a much more feasible possibility than preventing the production of all particles.

6. References

Bouchoule, A.; Plain, A.; Boufendi, L.; Biondeau, J. Ph.; Laure, C. (15 August 1991). "Particle Generation and Behavior in a Silane-Argon Low-Pressure Discharge Under Continuous or Pulsed Radio-Frequency Excitation," J. Appl. Phys. (70:4); pp. 1991-2000.

Fukuzawa, T.; Shiratani, M.; Watanabe, Y. (6 June 1994). "Novel *In Situ* Method to Detect Subnanometer-Sized Particles in Plasmas and its Application to Particles in Helium-Diluted Silane Radio Frequency Plasmas," Appl. Phys. Lett. (64:23); pp. 3098-3 100.

Gallagher, A.; Tanenbaum, D.; Laracuente, A.; Jalencovic,B (July 1995). *Atomic-Scale Characterization of Hydrogenated Amorphous-Silicon Films and Devices, Final Subcontract Report, 15 April, 1994-14 April 1995*, NREL/TP-411-8246. NTIS Accession No. DE ??. Golden, CO: National Renewable Energy Laboratory.

Howling, A.A.; Sansonnens, L.; Dorier, J.-L.; Hollenstein, Ch. (I February 1994). "Time-Resolved Measurements of Highly Polymerized Negative Ions in Radio Frequency Silane Plasma Deposition Experiments." J. Appl. Phys. (75:3); pp. 1340-1353, and references therein.

Schmidt, U.I.; Schrbder, B.; Oechsner, H. (I I December 1993). "Influence of Powder Formation in a Silane Discharge on a-Si:H Film Growth Monitored by *In Situ* Ellipsometry." J. Non-Cryst. Sol. 164-166,127(1993)

Silver, R. M.; Dagaata, J. A.; Tseng, W. (September-October 1995). "Dilineation of pn junctions by STM microscopy/spectroscopy in air and vacuum." J. Vac. Sci. Tech. A (13:5); pp. 1705-1713.

Smith, A.R.; Chao, K.-J.; Shih, C.K.; Shih, Y.C., Streetman, B.G. (23 January 1995). "Cross-Sectional Scanning Tunneling Microscopy Study of GaAs/AlAs Short Period Superlattices: The Influence of Growth Interrupt on the Interfacial Structure." Appi. Phys. Lett. (66:4); pp. 478-480.

Thibado, P. M.; Mercer, T. W.; Fu, S.; Egami, T.; DNardo, N. J.; and Bonnell, D. A. (March-April 1996). "Cross-sectioned STM spectroscopy of cleaved, Si-based MOS semiconductorjunctions." J. Vac. Sci. Tech. B (14:2), pp. 1607-1612.

Watanabe, Y.; Shiratani, M.; Makino, H. (I 5 October 1990). "Powder-Free Plasma Chemical Vapor Deposition of Hydrogenated Amorphous Silicon with High RF Power Density Using Modulated RF Discharge." Appl. Phys. Lett. (57:16); pp. 1616-1618.

REPORT DOCUMENTATION PAGE

Form Approved
OMB NO. 0704-0188

Public reporting burden for this collection of information is estimated to average 1 hour per response, including the time for reviewing instructions, searching existing data sources, gathering and maintaining the data needed, and completing and reviewing the collection of information. Send comments regarding this burden estimate or any other aspect of this collection of information, including suggestions for reducing this burden, to Washington Headquarters Services, Directorate for Information Operations and Reports, 1215 Jefferson Davis Highway, Suite 1204, Arlington, VA 22202-4302, and to the Office of Management and Budget, Paperwork Reduction Project (0704-0188), Washington, DC 20503.

1. AGENCY USE ONLY (Leave blank)	2. REPORT DATE	3. REPORT TYPE AND DATES COVERED
	February 1997	Annual Subcontract Report, 14 February 1995 - 14 April 1996

4. TITLE AND SUBTITLE

Atomic-Scale Characterization of Hydrogenated Amorphous-Silicon Films and Devices; Annual Subcontract Report, 14 February 1995 - 14 April 1996

5. FUNDING NUMBERS

C: DAD-4-14084-01
TA: PV704401

6. AUTHOR(S)

A. Gallagher, S. Barzen, M. Childs, and A. Laracuente

7. PERFORMING ORGANIZATION NAME(S) AND ADDRESS(ES)

National Institute of Standards and Technology
Boulder, Colorado 80303

8. PERFORMING ORGANIZATION REPORT NUMBER

9. SPONSORING/MONITORING AGENCY NAME(S) AND ADDRESS(ES)

National Renewable Energy Laboratory
1617 Cole Blvd.
Golden, CO 80401-3393

10. SPONSORING/MONITORING AGENCY REPORT NUMBER

SR-520-22565

DE97000210

11. SUPPLEMENTARY NOTES

NREL Technical Monitor: B. von Roedern

12a. DISTRIBUTION/AVAILABILITY STATEMENT	12b. DISTRIBUTION CODE
	UC-1262

13. ABSTRACT *(Maximum 200 words)*

Our research is concerned with improving the electronic properties of hydrogenated amorphous silicon (a-Si:H) films and of photovoltaic (PV) cells that use these films. Two approaches toward this goal are being taken. One is to establish the character of silicon particle growth in the rf glow discharges that are used to make the films and PV cells, and to understand the particle incorporation into the films. The ultimate goal of this effort is to find mitigating techniques that minimize the particle incorporation. During this contract period, we have developed a novel particle light-scattering technique that provides a very detailed and sensitive diagnostic of the particles suspended in the discharge, The second program is directed toward measuring the electronic properties of these thin-film PV cells, as a function of depth within the cell. The approach being taken is to use a scanning tunneling microscope to measure the depth-dependent electronic properties of cross-sectioned PV cells. During the present period, cell cleaving and cross-section locating methods, both in a ultrahigh vacuum environment, have been successfully developed.

14. SUBJECT TERMS

photovoltaics ; hydrogenated amorphous silicon films ; thin-film photovoltaic cells ; atomic-scale characterization

15. NUMBER OF PAGES
25

16. PRICE CODE

17. SECURITY CLASSIFICATION OF REPORT	18. SECURITY CLASSIFICATION OF THIS PAGE	19. SECURITY CLASSIFICATION OF ABSTRACT	20. LIMITATION OF ABSTRACT
Unclassified	Unclassified	Unclassified	UL